European Journal of Radiology 120 (2019) 108671

Contents lists available at ScienceDirect

European Journal of Radiology

journal homepage: www.elsevier.com/locate/ejrad

Research article

# Prognostic value of $^{18}$F-FDG PET/MR imaging biomarkers in oesophageal squamous cell carcinoma

Chih-Wei Yu[a], Xin-Jia Chen[b], Yen-Heng Lin[a], Yao-Hui Tseng[c], Ching-Chu Lu[d], Bang-Bin Chen[a], Shwu-Yuan Wei[a], Jang-Ming Lee[e,*], Tiffany Ting-Fang Shih[a,*]

[a] Department of Radiology and Medical Imaging, National Taiwan University College of Medicine and Hospital, No. 7, Chung-Shan South Rd, Taipei 10016, Taiwan
[b] Department of Medical Imaging, Sin-Lau Medical Foundation the Presbyterian Church in Taiwan, No. 57, Sec. 1, Dongmen Rd., East Dist., Tainan 70142, Taiwan
[c] Department of Medical Imaging, Cardinal Tien Hospital, No. 362, Zhongzheng Rd., Xindian Dist., New Taipei City 23148, Taiwan
[d] Department of Nuclear Medicine, National Taiwan University Hospital, No. 7, Chung-Shan South Rd., Taipei 10016, Taiwan
[e] Department of Surgery, National Taiwan University College of Medicine and Hospital, No. 7, Chung-Shan South Rd., Taipei 10016, Taiwan

ARTICLE INFO

*Keywords:*
Positron emission tomography
Magnetic resonance imaging
Oesophageal carcinoma
Diffusion-weighted imaging
Progression-free survival
Overall survival

ABSTRACT

*Purpose:* To correlate the clinical stage and prognosis of oesophageal squamous cell carcinoma (SCC) using the imaging biomarkers from integrated positron emission tomography (PET)/magnetic resonance imaging (MRI).
*Methods:* In total, 54 consecutive patients with oesophageal SCC who receive PET/MRI scan were recruited before treatment. The imaging biomarkers used were the mean and minimal apparent diffusion coefficients ($ADC_{mean}$ and $ADC_{min}$), standardized uptake value (SUV), metabolic tumour volume (MTV), and total lesion glycolysis (TLG) of tumours. The correlation between each imaging biomarker and survival was investigated using the Cox proportional hazards model.
*Results:* $ADC_{mean}$ was negatively correlated with $SUV_{max}$ ($r = -0.414$, $P = 0.025$). $ADC_{min}$ was negatively correlated with $SUV_{max}$ ($r = -0.423$, $P = 0.001$) and $SUV_{peak}$ ($r = -0.402$, $P = 0.003$), and was significantly lower in M1 than in M0 tumours (829.6 vs. 1069.8, $P = 0.005$). MTV was significantly higher in T3 + ($P < 0.001$), N1 + ($P = 0.014$) and TNM stage III + ($P < 0.001$) tumours. TLG was significantly higher in T3 + ($P < 0.001$), N1 + ($P < 0.001$), M1 ($P = 0.045$) and TNM stage III + ($P < 0.001$) tumours. The MTV/$ADC_{min}$ ratio exhibited the highest area under the receiver operating characteristic curve (AUROC) for predicting M1 and advanced TNM stage tumours. Multivariate analysis for progression-free survival (PFS) and overall survival (OS) showed that a larger MTV/$ADC_{min}$ was associated with a shorter PFS and OS ($P = 0.024$ and 0.046, respectively).
*Conclusion:* The imaging biomarkers in integrated PET/MRI may predict clinical stage and survival in patients with oesophageal SCC.

## 1. Introduction

Oesophageal cancer is the 6th leading cause of cancer-related death in the world [1]. Oesophageal cancer has two main histological types: squamous cell carcinomas and adenocarcinomas. For most of the 20th century, squamous cell carcinoma has predominated and is associated with a 5-year survival rate of 15%–25 % [2]. However, the incidence of adenocarcinoma of the oesophagus has been rising rapidly in the Western nations for the past three decades [3]. According to the 7th edition of the AJCC staging system for oesophageal cancer, published in 2010, histopathologic cell type defines staging classification [4].

Multimodality diagnosis using endoscopic ultrasound, contrast-enhanced computed tomography (CECT) of the neck, chest, and abdomen and whole-body $^{18}$F-fluorodeoxyglucose (FDG)-positron emission tomography (PET)/CT, is critical for staging before treatment of oesophageal cancer. Although $^{18}$F-FDG-PET/CT has limited value for regional tumour staging in oesophageal cancer, it is useful to detect distant lymphatic and haematogenous metastases [5,6]. The use of the $^{18}$F-FDG tracer in PET/CT allows for a quantitative assessment of cellular glucose metabolism in tumours by measuring the standardized uptake value (SUV). SUV of the primary tumour may serve as a prognostic factor in oesophageal cancer [7]. Furthermore, volume-based parameters such as metabolic tumour volume (MTV) and total lesion glycolysis (TLG) measured in $^{18}$F-PET/CT may be valuable as prognostic biomarkers in oesophageal cancer imaging [8–11].

Presently, the role of magnetic resonance imaging (MRI) in

* Corresponding authors.
*E-mail addresses:* jmlee@ntu.edu.tw (J.-M. Lee), ttfshih@ntu.edu.tw (T.T.-F. Shih).

https://doi.org/10.1016/j.ejrad.2019.108671
Received 18 March 2019; Received in revised form 5 September 2019; Accepted 12 September 2019

oesophageal cancer staging and treatment response assessment is limited [12]. The apparent diffusion coefficient (ADC) measured using diffusion-weighted imaging (DWI) may be useful in predicting response to neoadjuvant chemoradiotherapy (CRT) in oesophageal cancer [13,14]. Furthermore, ADC may also be a potent prognostic factor for oesophageal cancer patients receiving CRT [15,16].

Integrated $^{18}$F-PET/MRI can provide comprehensive information for cancer staging in patients [17]. Functional information, including ADC values from DWI and glycolytic activity from PET, can be obtained through $^{18}$F-PET/MRI during a single examination. To date, studies on $^{18}$F-PET/MRI in oesophageal cancer staging have been limited [18]. For oesophageal cancer, combination of function parameters obtained using $^{18}$F-PET/MRI may be useful for tumour staging and predicting patient outcome.

The aim of this study was to evaluate the correlation between clinical TNM stage and prognosis in patients with oesophageal carcinoma and imaging biomarkers obtained from $^{18}$F-PET/MRI.

## 2. Materials and methods

### 2.1. Patients

This prospective study was approved by the institutional review board of our hospital, and informed consent was obtained from all participating patients. Consecutive patients scheduled for whole-body $^{18}$F-FDG PET/CT for the staging of clinically indicated oesophageal squamous cell carcinoma were identified and invited to participate in the study. The patients were administered an intravenous injection of $^{18}$F-FDG and subjected to PET/CT, immediately followed by PET/MRI with the residual positron activity from the initial injection.

From May 2014 to August 2017, 54 consecutive patients (mean age 60.6 ± 11.7 years, range: 41–84 years; 49 men and 5 women) were enrolled for PET/CT and PET/MRI examinations before treatment. Inclusion criteria were presence of pathologically confirmed oesophageal squamous cell carcinoma examined by EUS-guided biopsy, presence of a clinical indication for staging, and stable medical condition. Exclusion criteria were a history of malignancy, surgery or radiotherapy to the mediastinum, pregnancy, renal insufficiency, or contraindication to MRI. Patient characteristics are presented in Table 1.

**Table 1**
Clinical information of the 54 patients with oesophageal carcinoma.

| Characteristic | Data |
|---|---|
| Age (years) | 60.6 ± 11.7 (41–84) |
| Gender (M/F) | 49/5 |
| Tumour location | |
| Cervical | 2 (3.7) |
| Upper third | 12 (22.2) |
| Middle third | 17 (31.5) |
| Lower third | 23 (42.6) |
| T stage | |
| T1 | 4 (7.4) |
| T2 | 6 (11.1) |
| T3 | 40 (74.1) |
| T4 | 4 (7.4) |
| N stage | |
| N0 | 4 (7.4) |
| N1 | 19 (35.2) |
| N2 | 21 (38.9) |
| N3 | 10 (18.5) |
| M stage | |
| M0 | 37 (68.5) |
| M1 | 17 (31.5) |
| TNM stage | |
| I | 1 (1.9) |
| II | 8 (14.8) |
| III | 28 (51.9) |
| IV | 17 (31.5) |

The data presented are means ± standard deviation (range), or number (percentage) of patients.

### 2.2. PET/MRI protocol

Each patient was required to fast for more than 6 h, and blood glucose levels were verified to be less than 200 mg/dL (< 11.1 m mol/L) before PET/CT. The scan was performed using a Discovery ST PET/CT scanner (GE Medical Systems, Milwaukee, WI, USA) 50 min after the intravenous injection of $^{18}$F-FDG at 5 MBq/kg (0.14 m Ci/kg). All patients were transferred to a 3.0 Tesla PET/MRI scanner (Biograph mMR; Siemens Healthcare, Erlangen, Germany) located in the same building immediately after the PET/CT examination, at a mean interval of 105 min (88–147 min) following the initial FDG injection.

PET was performed from the head to mid-thighs in 5 bed positions (acquisition time: 4 min per position) with the patient in the supine position. The images were reconstructed using an ordered-subsets expectation-maximization iterative algorithm (2 iterations, 21 subsets) with a 5-mm post-reconstruction Gaussian filter and an image matrix of 172 × 172 pixels. The attenuation correction of the PET data was performed using a four-tissue (air, lung, fat and soft tissue) segmented attenuation map acquired with a two-point Dixon MRI sequence.

The MR protocol for each patient included pre-contrast whole-body, dedicated thoracic, and post-contrast whole-body scans. Simultaneous whole-body MRI with coronal STIR (repetition time [TR]/echo time [TE]: 5,000/51 ms, flip angle [FA]: 120°, slice thickness/gap: 6/0.6 mm, matrix size: 256 × 192, FOV: 450 × 302 mm, and number of excitations [NEX]: 1), coronal T2-weighted half-Fourier-acquired single-shot turbo spin echo (HASTE; TR/TE: 1,500/87 ms, FA: 90°, slice thickness/gap: 6/0.6 mm, matrix size: 384 × 258, FOV: 450 × 302 mm, and NEX: 1), and axial T2-weighted HASTE (TR/TE: 1,500/84 ms, FA: 140°, slice thickness: 5 mm, matrix size: 320 × 320, FOV: 350 × 350 mm, NEX: 1; Fig. 1A) were performed while acquiring PET data in each bed position. Following the simultaneous PET/MRI data acquisition, the mediastinum was subjected to dedicated thoracic scanning, namely sagittal T2-weighted HASTE (TR/TE: 1,500/84 ms, FA: 130°, slice thickness: 5 mm, matrix size: 416 × 512, FOV: 276 × 340 mm, and NEX: 1), axial Dixon T1 volumetric interpolated breath-hold examination (VIBE) with and without fat saturation (TR/TE: 3.1/1.2 ms, FA: 70°, slice thickness: 3 mm, matrix size: 640 × 240, FOV: 300 × 253 mm, and NEX: 1), axial respiratory-triggered T2-weighted fast spin-echo sequence (TR/TE: 2,900/85 ms, FA: 126°, slice thickness: 3 mm, matrix size: 512 × 512, FOV: 250 × 250 mm, and NEX: 3), and axial DWI (TR/TE: 7,000/79 ms, FA: 90°, slice thickness: 5 mm, matrix size: 320 × 272, FOV: 380 × 323 mm, and NEX: 3; b = 0, 50, 800; Fig. 1B). The ADC maps were calculated with a mono-exponential function (b values 0, 50 and 800 s/mm2; Fig. 1C). The total scan duration was 60–70 min.

### 2.3. Image analysis

Two experienced radiologists independently measured ADC and PET parameters of the primary tumours using imaging software (syngo.via; Siemens Healthcare, Erlangen, Germany) and interobserver reliability was evaluated. One nuclear medicine physician examined the PET/MR images to evaluate lymph nodes and distant metastasis. For ADC measurements ($ADC_{mean}$ and $ADC_{min}$), regions of interest (ROIs) were manually drawn on ADC maps along the tumour contour on a single slice from the largest area of the tumour. ROIs were 6.1 ± 3.0 $cm^2$ (range 1.2–14.7 $cm^2$).

Relevant PET-related parameters measured were $SUV_{max}$, which reflected the maximal SUV (adjusted for body weight); $SUV_{peak}$, which represented the computationally automated maximal average SUV in a 1-$cm^3$ spherical volume within a tumour; MTV, expressed as the tumour volume with FDG uptake, which was segmented using a fixed-

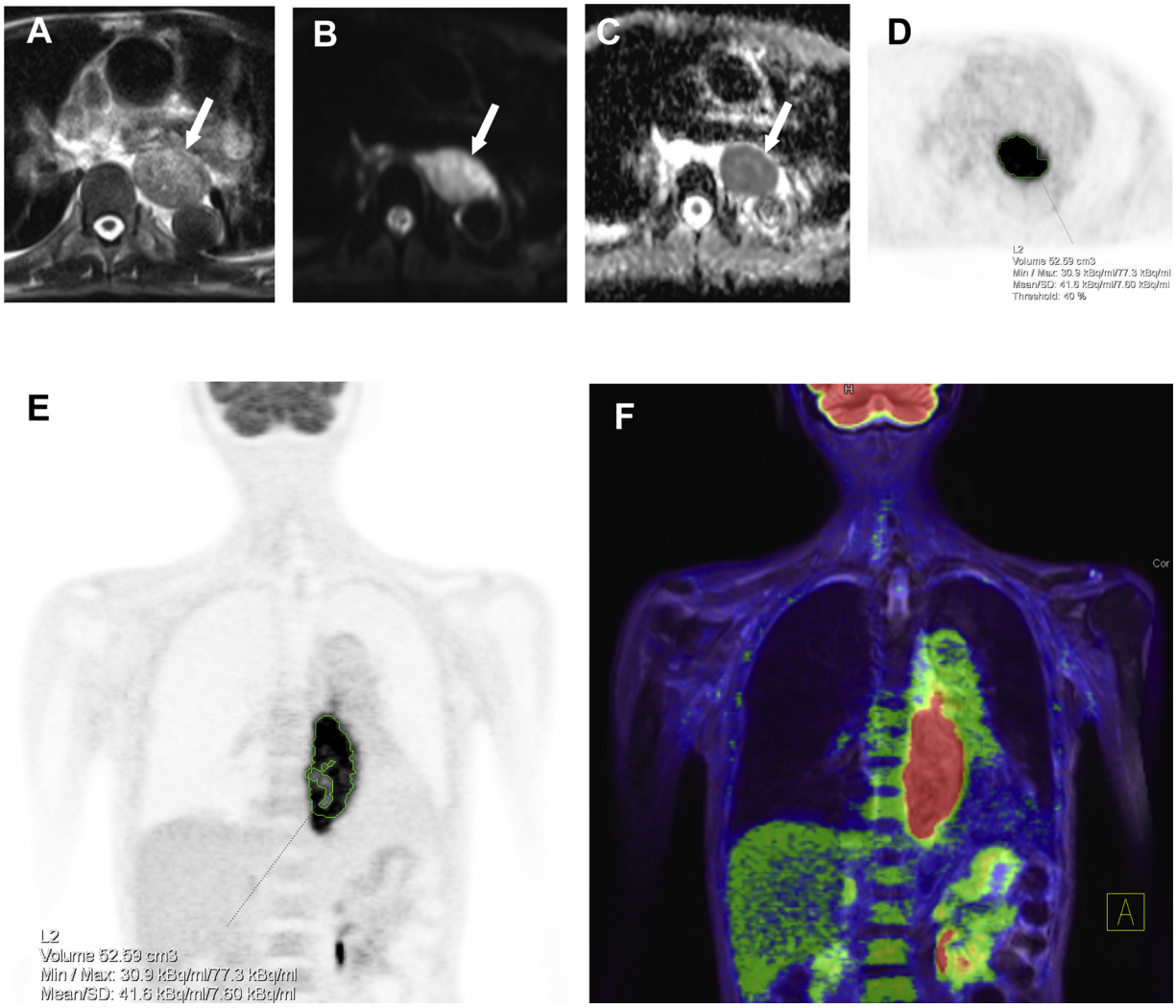


**Fig. 1.** Images of a 77-year-old man with oesophageal carcinoma (T3N1M0, stage 3). **(A)** Axial T2- weighted MR shows that the tumour is hyperintense (arrow). (B) Axial diffusion-weighted MR shows that the tumour is hyperintense (arrow). (C) Axial ADC map shows that the tumour is hypointense (arrow), which corresponds with the low ADC values. Axial PET (D) and coronal PET (E) show high glucose metabolic activity and metabolic tumour volume (green line, threshold = 40%) of the tumour. (F) Coronal fused PET/MR shows high glucose metabolic activity of the tumour.

percentage threshold method at 40% of the $SUV_{max}$ (Fig. 1D and E); and TLG, the product of MTV and the average SUV of the included voxels. The fixed-threshold MTV and TLG were automatically derived from these tumour delineations using a software (available as a predefined syngo.via tool).

### 2.4. Clinical TNM classification, treatment and follow-up

TNM staging was classified according to the 7th edition of the American Joint Committee on Cancer TNM classification based on information obtained regarding the tumour during tumour surgery and histological or imaging studies.

Among the 54 patients, 24 underwent treatment without surgery: specifically, 18 received definitive chemoradiation; 4 received chemotherapy; and 2 received radiation. The remaining patients (n = 30) received surgical resection and reconstruction of the oesophagus. Of these patients, 8 underwent surgery only; 1 received chemotherapy in addition to surgery; and 21 received cisplatin-based neoadjuvant chemoradiotherapy (CRT) followed by oesophagectomy.

All patients underwent imaging (CECT or MRI) 1 month after completing treatment and subsequently every 3–6 months. Overall survival (OS) duration was defined as the interval between the initial diagnosis or oesophagectomy (for surgical patients) and mortality of the patient. Progression-free survival (PFS) was defined as the interval between the initial diagnosis or oesophagectomy and detection of recurrence or metastasis or death from the disease. The final data collection date was 30 June 2018, and patients in whom no event occurred or who were lost to follow-up were excluded accordingly.

### 2.5. Statistical analysis

Summary statistics are presented as mean ± standard deviations for continuous variables and frequency and percentage for categorical variables. Statistical analyses were performed using SPSS version 22 (IBM Corp., Armonk, NY). Pearson correlation coefficients were calculated to evaluate the relationships between imaging biomarkers as well as the differences between the imaging biomarkers with respect to TNM stage. Optimal cut-off values, sensitivity, and specificity of the imaging biomarkers for differentiating TNM stages were determined using area under the receiver operating characteristic curve and the Youden index. Interobserver reliability was calculated using the intraclass correlation coefficient.

PFS and OS were estimated using the Kaplan–Meier method. The log-rank test was used to assess the difference in PFS between groups, and the median values of variables were used as cut-off values. Furthermore, Cox proportional hazards regression was used to assess

**Table 2**
Correlations between MRI- and PET-derived biomarkers.

| | | $ADC_{mean}$ | $ADC_{min}$ | $SUV_{max}$ | $SUV_{peak}$ | MTV | TLG |
|---|---|---|---|---|---|---|---|
| $ADC_{mean}$ | Correlation (r) | 1 | 0.760 | −0.414 | −0.441 | −0.245 | −0.300 |
| | *p* value | | < 0.001* | 0.025* | 0.067 | 0.205 | 0.103 |
| $ADC_{min}$ | Correlation (r) | | 1 | −0.423 | −0.402 | −0.205 | −0.234 |
| | *p* value | | | 0.001* | 0.003* | 0.137 | 0.088 |
| $SUV_{max}$ | Correlation (r) | | | 1 | 0.973 | 0.196 | 0.445 |
| | *p* value | | | | < 0.001* | 0.155 | 0.001* |
| $SUV_{peak}$ | Correlation (r) | | | | 1 | 0.246 | 0.489 |
| | *p* value | | | | | 0.072 | < 0.001* |
| MTV | Correlation (r) | | | | | 1 | 0.924 |
| | *p* value | | | | | | < 0.001* |
| TLG | Correlation (r) | | | | | | 1 |
| | *p* value | | | | | | |

* $p < 0.05$.

the relationship between PFS, OS, and other covariates, including age, gender, tumour size, and tumour stage. A *P* value < 0.05 was considered statistically significant.

## 3. Results

### 3.1. Correlations between MRI- and PET-derived biomarkers

The correlations between $ADC_{mean}$, $ADC_{min}$, $SUV_{max}$, $SUV_{peak}$, MTV and TLG are summarized in Table 2. ADC was negatively correlated with SUV. Among MRI-derived biomarkers, $ADC_{min}$ showed higher correlation with SUV than $ADC_{mean}$. Among PET-derived biomarkers, SUV was positively correlated with MTV and TLG.

### 3.2. Associations between imaging biomarkers and clinical TNM stage

The associations between $ADC_{mean}$, $ADC_{min}$, $SUV_{max}$, $SUV_{peak}$, MTV, TLG, MTV/ $ADC_{min}$ and T, N, M and TNM stages are summarized in Table 3. No significant correlation was detected between $ADC_{mean}$ and clinical stages. $ADC_{min}$ was significantly lower whereas $SUV_{max}$ and $SUV_{peak}$ were significantly higher in high T stage (T3 + ) tumours. MTV, TLG and MTV/$ADC_{min}$ ratios were all significantly higher in advanced stage (T3 + , N1 + , and TNM stage III + ) tumours.

### 3.3. Predictive values of imaging biomarkers for predicting T, N, M and TNM stages

The predictive values of $ADC_{min}$, MTV, TLG, and MTV/ $ADC_{min}$ for predicting T, N, M and TNM stages are summarized in Table 4. Since better correlation between clinical TNM staging and $ADC_{min}$ than $ADC_{mean}$, as well as better correlation between clinical TNM staging and MTV than SUV parameters, was found, we used $ADC_{min}$, MTV, TLG and MTV/$ADC_{min}$ ratio for further comparison. Table 4 showed the optimal cut-off values, sensitivity and specificity of $ADC_{min}$, MTV, TLG and MTV/$ADC_{min}$ ratio in relation to the T, N, M and TNM stages. Among these biomarkers, TLG exhibited the highest AUROC for predicting T stage (stage ≦ 2 vs. ≧ 3, AUROC = 0.802; Fig. 2A) and MTV exhibited the highest AUROC for predicting N stage (stage 0 vs. ≧ 1, AUROC = 0.735; Fig. 2B). Compared with $ADC_{min}$ or MTV or TLG, MTV/$ADC_{min}$ ratio exhibited the highest AUROC for predicting M stage (stage 0 vs. 1, AUROC = 0.774) and advanced TNM stage (stage ≤ II vs. ≥ III, AUROC = 0.815) (Fig. 2C and D).

### 3.4. Interobserver reliability

The ICCs (95% confidence interval) for assessing the interobserver reliability of measuring were 0.824 (0.775–0.887) for $ADC_{mean}$ indicating good agreement between the two observers. The ICCs (95%

**Table 3**
Associations between imaging biomarkers and clinical TNM stage.

| | T stage | | | N stage | | | M stage | | |
|---|---|---|---|---|---|---|---|---|---|
| | ≦ 2 (N = 10) | ≧ 3 (N = 44) | *p* value | 0 (N = 4) | ≧ 1 (N = 50) | *p* value | 0 (N = 37) | 1 (N = 17) | *p* value |
| ADCmean (×10–6 mm2/s) | 1504.6 ± 529.5 | 1336.4 ± 350.8 | 0.273 | 1109.6 ± 377.1 | 1391.3 ± 439.2 | 0.376 | 1376.4 ± 463.0 | 1330.9 ± 403.1 | 0.747 |
| ADCmin (×10–6 mm2/s) | 1272.3 ± 445.6 | 931.0 ± 267.9 | 0.033* | 861.3 ± 397.0 | 1004.8 ± 384.4 | 0.476 | 1069.8 ± 430.5 | 829.6 ± 366.7 | 0.005* |
| SUVmax | 11.9 ± 6.7 | 20.0 ± 9.6 | 0.015* | 17.9 ± 6.3 | 18.5 ± 9.9 | 0.902 | 17.6 ± 10.4 | 20.4 ± 7.6 | 0.320 |
| SUVpeak | 8.6 ± 5.3 | 14.1 ± 7.4 | 0.030* | 11.7 ± 3.1 | 13.2 ± 7.6 | 0.700 | 12.5 ± 8.1 | 14.4 ± 5.3 | 0.382 |
| MTV (mL) | 3.8 ± 2.3 | 17.7 ± 19.1 | < 0.001* | 4.6 ± 5.2 | 16.0 ± 18.1 | 0.014* | 12.0 ± 14.8 | 22.0 ± 19.8 | 0.112 |
| TLG | 28.9 ± 30.2 | 218.8 ± 230.9 | < 0.001* | 39.0 ± 30.2 | 195.2 ± 211.1 | < 0.001* | 135.0 ± 148.1 | 289.5 ± 326.5 | 0.045* |
| MTV/ADCmin ($\times 10^3$) | 3.9 ± 3.7 | 21.7 ± 23.6 | < 0.001* | 5.0 ± 3.9 | 19.5 ± 21.4 | 0.002* | 13.7 ± 15.1 | 28.7 ± 26.6 | 0.063 |

| | TNM stage | | |
|---|---|---|---|
| | ≦ II (N = 9) | ≧ III (N = 45) | *p value* |
| ADCmean (×10–6 mm2/s) | 1453.8 ± 554.1 | 1347.4 ± 370.9 | 0.457 |
| ADCmin (×10–6 mm2/s) | 1184.6 ± 494.1 | 956.1 ± 351.7 | 0.103 |
| SUVmax | 13.8 ± 7.4 | 19.4 ± 9.8 | 0.109 |
| SUVpeak | 9.2 ± 4.6 | 13.8 ± 7.6 | 0.085 |
| MTV (mL) | 3.7 ± 3.7 | 17.4 ± 20.8 | < 0.001* |
| TLG | 27.3 ± 24.5 | 214.9 ± 249.1 | < 0.001* |
| MTV/ADCmin ($\times 10^3$) | 3.4 ± 3.0 | 21.5 ± 24.3 | < 0.001* |

The data presented are means ± standard deviation.
* $p < 0.05$; Student's *t*-test for T, N, M and TNM stages.

**Table 4**
Predictive values of imaging biomarkers for predicting T, N, M and TNM stages.

| Biomarkers | $ADC_{min}$ ($\times 10^{-6}$ mm2/s) | MTV (mL) | TLG | $MTV/ADC_{min}$ ($\times 10^{3}$) |
|---|---|---|---|---|
| T stage (≦2 vs. ≧3) | | | | |
| Cut-off value | 940 | 8.2 | 43.4 | 7.5 |
| Sensitivity (%) | 61.4 | 54.5 | 75.0 | 63.6 |
| Specificity (%) | 70.0 | 100.0 | 90.0 | 90.0 |
| AUROC | 0.655 (0.513–0.779) | 0.764 (0.628– 0.869) | 0.802 (0.671– 0.898) | 0.782 (0.648– 0.883) |
| *p* value | 0.038* | < 0.001* | < 0.001* | < 0.001* |
| N stage (0 vs. ≧1) | | | | |
| Cut-off value | 600 | 3.7 | 80.3 | 9.1 |
| Sensitivity (%) | 94.0 | 72.0 | 54.0 | 52.0 |
| Specificity (%) | 50.0 | 75.0 | 100.0 | 100.0 |
| AUROC | 0.605 (0.463 – 0.735) | 0.735 (0.597–0.846) | 0.690 (0.550–0.809) | 0.703 (0.563–0.819) |
| *p* value | 0.624 | 0.093 | 0.023* | 0.064 |
| M stage (0 vs. 1) | | | | |
| Cut-off value | 1020 | 12.3 | 91.4 | 12.7 |
| Sensitivity (%) | 100.0 | 64.7 | 76.5 | 70.6 |
| Specificity (%) | 43.2 | 81.1 | 67.6 | 75.7 |
| AUROC | 0.672 (0.530–0.793) | 0.746 (0.610– 0.855) | 0.749 (0.612– 0.857) | 0.774 (0.640– 0.877) |
| *p* value | 0.019* | 0.001* | < 0.001* | < 0.001* |
| TNM stage (≦II vs. ≧III) | | | | |
| Cut-off value | 968 | 3.7 | 43.4 | 9.1 |
| Sensitivity (%) | 66.7 | 77.8 | 73.3 | 57.8 |
| Specificity (%) | 77.8 | 77.8 | 88.9 | 100.0 |
| AUROC | 0.664 (0.523– 0.787) | 0.800 (0.699– 0.896) | 0.810 (0.680– 0.904) | 0.815 (0.686– 0.907) |
| *p* value | 0.197 | < 0.001* | < 0.001* | < 0.001* |

* $p < 0.05$.

confidence interval) for assessing the interobserver reliability of measuring were and 0.913 (0.868–0.966) for $ADC_{min}$, 0.999 (0.995–1) for $SUV_{max}$, 0.999 (0.997–1) for $SUV_{peak}$, 0.980 (0.960–0.995) for TLG, and 0.994 (0.990–1) for MTV, indicating excellent agreement between the two observers.

### 3.5. Univariate and multivariate analysis of parameters with clinical outcome

The median follow-up in all patients was 1152 days (range 330–1508 days). Because the $MTV/ADC_{min}$ ratio exhibited highest AUROC for predicting tumour stage, we used it as the imaging biomarker for predicting PFS and OS. The univariate and multivariate analysis of age, gender, tumor location, TNM stage and $MTV/ADC_{min}$ ratio with PFS and OS are summarized in Table 5. In the univariate analysis, a higher TNM stage and a higher $MTV/ADC_{min}$ were associated with a shorter PFS (hazard ratio = 3.354 and 3.598, respectively) and a higher TNM stage and a higher $MTV/ADC_{min}$ were associated with a shorter OS (hazard ratio = 4.807 and 3.352, respectively). In the multivariate analysis, a higher $MTV/ADC_{min}$ was associated with a shorter PFS (hazard ratio = 2.577; Fig. 3A) and a higher $MTV/ADC_{min}$ was associated with a shorter OS (hazard ratio = 2.224; Fig. 3B). The other parameters were not significantly related to PFS or OS.

## 4. Discussion

We demonstrated that PET/MRI provides useful imaging biomarkers for clinical staging and predicts outcomes in patients with oesophageal squamous cell carcinoma. In our study, $ADC_{mean}$ and $ADC_{min}$ were inversely correlated with $SUV_{max}$. Tumours with high MTV were at more advanced T and N stages and were at an advanced TNM stage. Tumours with high TLG were at more advanced T, N, and M stages and were at an advanced TNM stage. Moreover, the $MTV/ADC_{min}$ ratio demonstrated the strongest predictive ability for determining the clinical TNM stage. After adjustment for age, gender, tumour location and TNM stage, the $MTV/ADC_{min}$ ratio was found to be an independent predictor of PFS and OS after treatment. Thus, integrated PET/MRI could provide complementary information on tumour characteristics and patient outcome.

Although DWI and FDG-PET reveal distinct tissue properties, the results obtained from these methods might be interrelated because of increased cellularity and glucose metabolism in cancers. Previous studies found no correlation between pre-treatment tumor ADC and SUV values in head and neck squamous cell carcinoma. Significant inverse correlation was found between ADC and SUV in different tumours and cancers [19–21]. By contrast, a recent study demonstrated that no significant correlation existed between tumour ADC and SUV obtained using MRI and PET/CT separately in patients with oesophageal cancer [22]. In our study, $ADC_{mean}$ and $ADC_{min}$ of primary tumours were inversely correlated with $SUV_{max}$. Acquisition of ADC and SUV together in integrated PET/MRI is advantageous because it enables correlation between 2 biomarkers simultaneously.

Our results revealed that $ADC_{min}$ was significantly lower in tumour stage ≧T3 than in tumour stage < T2. Similarly, a previous study showed an inverse correlation between ADC and oesophageal tumour stroma and angiogenesis [23]. In gastric cancer, both the preoperative $ADC_{min}$ and $ADC_{mean}$ values have been found correlated with the postoperative T staging [24]. In the present study, poor correlation between $ADC_{mean}$ and T stages suggested a better diagnostic value for tumour staging in $ADC_{min}$ than $ADC_{mean}$ in oesophageal cancer. The ADC value has also been observed as a prognostic factor for oesophageal cancer [25,26]. The survival rate in the high-ADC group was significantly better than that in the low-ADC group in this study.

The SUV is the most frequently used PET parameter for prognostic investigations in cancers. A meta-analysis reported that the SUV value measured on PET/CT is an effective predictor of outcome for patients with oesophageal cancer [7]. Most related studies have reported that high SUV before treatment predicted relatively poor OS. However, 2 large prospective trials reported that the initial PET $SUV_{max}$ did not predict survival in patients with locally advanced oesophageal cancer [27,28]. SUV estimates involve potential bias introduced by the partial volume effect from small lesions [29,30]; thus, for patient outcomes for many malignancies, volume-based parameters are more accurate predictors than is tumour $SUV_{max}$ [31–33]. Recent studies have demonstrated that MTV, a volume-based parameter of PET-CT, exhibits greater prognostic accuracy than $SUV_{max}$ and provides valuable prognostic information in oesophageal cancer [10,34]. Furthermore, our results suggested that volume-based parameters, including TLG and

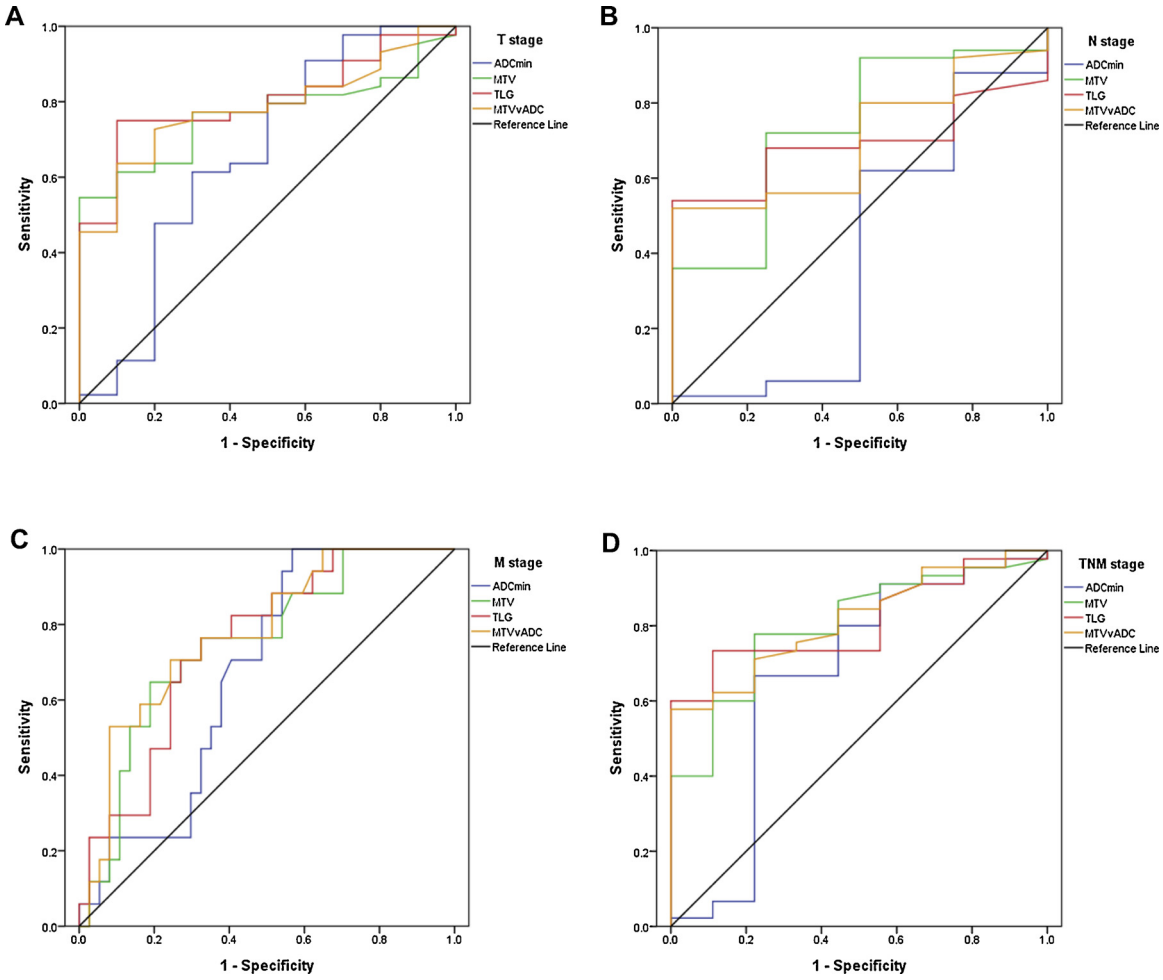


**Fig. 2.** Area under the receiver operating characteristic curves (AUROC) to evaluate the performance of $ADC_{min}$, MTV, TLG and $MTV/ADC_{min}$ ratio in differentiating T, N, M and TNM stages in 54 patients with oesophageal carcinoma. TLG showed the highest AUROC for predicting T stage (A stage ≦ 2 vs. ≧ 3, AUROC = 0.802), compared with $ADC_{min}$, MTV, and $MTV/ADC_{min}$ ratio. MTV showed the highest AUROC for predicting N stage (B stage 0 vs. ≧ 1, AUROC = 0.735), compared with $ADC_{min}$, TLG, and $MTV/ADC_{min}$ ratio. $MTV/ADC_{min}$ ratio showed the highest AUROC for predicting M stage (**C** stage 0 vs. 1, AUROC = 0.774), and advanced TNM stage (D stage ≦ II vs. ≧ III, AUROC = 0.815), compared with $ADC_{min}$, MTV, and TLG.

MTV, can provide valuable information to supplement that provided by SUV for predicting the clinical stage in patients with oesophageal cancer.

Combined parameter using ADC and SUV derived from $^{18}$F-FDG-PET/MRI has been used for different cancers. $SUV_{max}/ADC_{min}$ ratio has been found correlated with average nucleic area in head and neck squamous cell carcinoma [35]. Similarly, $MTV/ADC_{min}$ ratio may predict clinical stage and PFS in patients with pancreatic or periampullary cancer [36]. In our study, the $MTV/ADC_{min}$ ratio demonstrated the greatest predictive value for determining the clinical TNM stage and was an independent predictor of PFS and OS. Because both ADC and MTV are prognostic imaging biomarkers in oesophageal cancer, use of integrated PET/MRI is advantageous because this strategy enables investigation of both of these imaging biomarkers in a

**Table 5**
Univariate and multivariate analysis of parameters with clinical outcome.

| Parameters | Univariate | | | Multivariate | | |
|---|---|---|---|---|---|---|
| | Hazard ratio | 95 % CI | *p* value | Hazard ratio | 95 % CI | *p* value |
| Progression-free survival | | | | | | |
| Age (≧60 vs. < 60 years) | 1.232 | 0.615–2.466 | 0.556 | 1.206 | 0.550–2.646 | 0.640 |
| Gender (female vs. male) | 4.141 | 0.563– 30.453 | 0.163 | 2.080 | 0.254– 17.054 | 0.495 |
| Location (upper 2/3 vs. lower1/3) | 1.738 | 0.866– 3.489 | 0.120 | 1.561 | 0.689–3.535 | 0.286 |
| TNM stage (≧III vs. ≦II) | 3.354 | 1.017– 11.063 | 0.047* | 2.106 | 0.541–8.205 | 0.183 |
| $MTV/ADC_{min}$ (≧9.1 vs. < 9.1) | 3.598 | 1.742– 7.434 | < 0.001* | 2.577 | 1.133–5.863 | 0.024* |
| Overall survival | | | | | | |
| Age (≧60 vs. < 60 years) | 1.068 | 0.538– 2.116 | 0.852 | 1.061 | 0.492–2.284 | 0.881 |
| Gender (female vs. male) | 4.410 | 0.602– 32.312 | 0.144 | 2.495 | 0.317– 19.620 | 0.385 |
| Location (upper 2/3 vs. lower1/3) | 1.474 | 0.744– 2.920 | 0.267 | 1.360 | 0.620–2.984 | 0.443 |
| TNM stage (≧III vs. ≦II) | 4.807 | 1.148– 20.132 | 0.032* | 3.039 | 0.638– 14.486 | 0.163 |
| $MTV/ADC_{min}$ (≧9.1 vs. < 9.1) | 3.352 | 1.639– 6.855 | < 0.001* | 2.224 | 1.015–4.873 | 0.046* |

* $p < 0.05$.

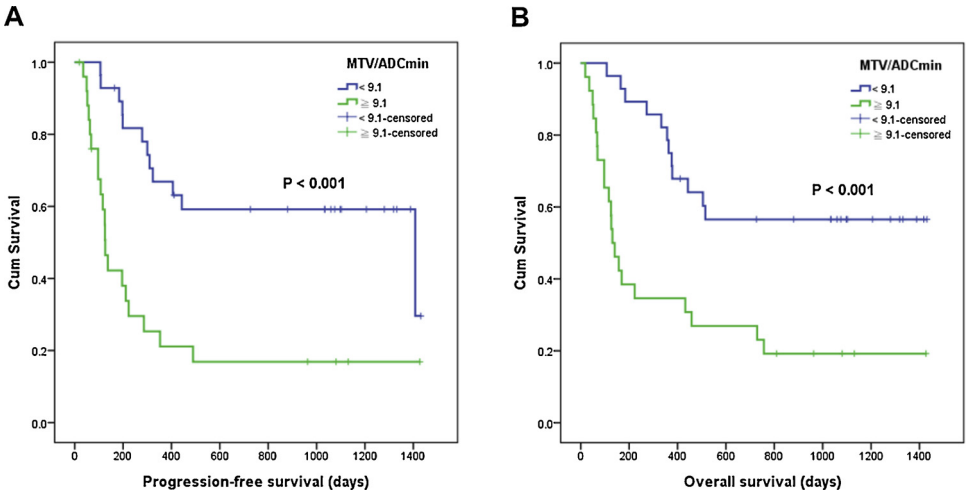


**Fig. 3.** Kaplan-Meier survival curves for progression-free survival (PFS) and overall survival (OS). (A) Patients with high values of MTV/$ADC_{min}$ ratio have shorter PFS than those with low values. (B) Patients with high values of MTV/$ADC_{min}$ ratio have shorter OS than those with low values.

single examination.

Our study had limitations. First, delayed PET data obtained on PET/MRI scanner after competition of prior PET/CT study may have potential influence on image quality due to tracer redistribution and decay. Second, the study cohort was relatively small, which may have resulted in type 2 errors and the non-significance of some results. Thus, a larger cohort of patients is necessary to validate our findings.

## 5. Conclusions

In conclusion, the combined data derived from DWI and PET provides complementary information on tumour characteristics in patients with oesophageal cancer. The combined parameter MTV/$ADC_{min}$ ratio is a powerful biomarker for determining clinical stage and outcome in these patients.

## Declaration of Competing Interest

All authors have no conflict of interest to disclose.

## Acknowledgements

The study was funded by National Taiwan University Hospital, Taipei, Taiwan; Contract grant number: A1 project no. NTUH103-A124.

## References

[1] J. Ferlay, I. Soerjomataram, R. Dikshit, S. Eser, C. Mathers, M. Rebelo, D.M. Parkin, D. Forman, F. Bray, Cancer incidence and mortality worldwide: sources, methods and major patterns in GLOBOCAN 2012, Int. J. Cancer 136 (5) (2015) E359–E386.
[2] A. Pennathur, M.K. Gibson, B.A. Jobe, J.D. Luketich, Oesophageal carcinoma, Lancet 381 (9864) (2013) 400–412.
[3] E. Bollschweiler, E. Wolfgarten, C. Gutschow, A.H. Holscher, Demographic variations in the rising incidence of esophageal adenocarcinoma in white males, Cancer 92 (3) (2001) 549–555.
[4] T.W. Rice, E.H. Blackstone, V.W. Rusch, 7th edition of the AJCC cancer staging manual: esophagus and esophagogastric junction, Ann. Surg. Oncol. 17 (7) (2010) 1721-4.
[5] H.L. van Westreenen, M. Westerterp, P.M. Bossuyt, J. Pruim, G.W. Sloof, J.J. van Lanschot, H. Groen, J.T. Plukker, Systematic review of the staging performance of 18F-fluorodeoxyglucose positron emission tomography in esophageal cancer, J. Clin. Oncol. 22 (18) (2004) 3805–3812.
[6] E.P. van Vliet, M.H. Heijenbrok-Kal, M.G. Hunink, E.J. Kuipers, P.D. Siersema, Staging investigations for oesophageal cancer: a meta-analysis, Br. J. Cancer 98 (3) (2008) 547–557.
[7] L. Pan, P. Gu, G. Huang, H. Xue, S. Wu, Prognostic significance of SUV on PET/CT in patients with esophageal cancer: a systematic review and meta-analysis, Eur. J. Gastroenterol. Hepatol. 21 (9) (2009) 1008–1015.
[8] C. Van de Wiele, V. Kruse, P. Smeets, M. Sathekge, A. Maes, Predictive and prognostic value of metabolic tumour volume and total lesion glycolysis in solid tumours, Eur. J. Nucl. Med. Mol. Imaging 40 (2) (2013) 290–301.
[9] S.Y. Park, S.J. Lee, J.K. Yoon, The prognostic value of total lesion glycolysis via 18F-fluorodeoxyglucose PET-CT in surgically treated esophageal squamous cell carcinoma, Ann. Nucl. Med. 30 (1) (2016) 81–88.
[10] D. Tamandl, J. Ta, R. Schmid, M. Preusser, M. Paireder, S.F. Schoppmann, A. Haug, A. Ba-Ssalamah, Prognostic value of volumetric PET parameters in unresectable and metastatic esophageal cancer, Eur. J. Radiol. 85 (3) (2016) 540–545.
[11] C. Lemarignier, F. Di Fiore, C. Marre, S. Hapdey, R. Modzelewski, P. Gouel, P. Michel, B. Dubray, P. Vera, Pretreatment metabolic tumour volume is predictive of disease-free survival and overall survival in patients with oesophageal squamous cell carcinoma, Eur. J. Nucl. Med. Mol. Imaging 41 (11) (2014) 2008-16.
[12] P.S. van Rossum, R. van Hillegersberg, F.M. Lever, I.M. Lips, A.L. van Lier, G.J. Meijer, M.S. van Leeuwen, M. van Vulpen, J.P. Ruurda, Imaging strategies in the management of oesophageal cancer: what's the role of MRI? Eur. Radiol. 23 (7) (2013) 1753–1765.
[13] S.E. Heethuis, L. Goense, P.S.N. van Rossum, A.S. Borggreve, S. Mook, F.E.M. Voncken, A. Bartels-Rutten, B.M.P. Aleman, R. van Hillegersberg, J.P. Ruurda, G.J. Meijer, J.J.W. Lagendijk, A. van Lier, DW-MRI and DCE-MRI are of complementary value in predicting pathologic response to neoadjuvant chemoradiotherapy for esophageal cancer, Acta Oncol. (2018) 1–8.
[14] B. Cheng, J. Yu, Predictive value of diffusion-weighted MR imaging in early response to chemoradiotherapy of esophageal cancer: a meta-analysis, Dis. Esophagus 32 (4) (2018) doy065.
[15] S. Liu, F. Zhen, N. Sun, J. Chen, Y. Cao, S. Zhang, H. Cheng, X. Ge, X. Sun, Apparent diffusion coefficient values detected by diffusion-weighted imaging in the prognosis of patients with locally advanced esophageal squamous cell carcinoma receiving chemoradiation, OncoTargets Ther. 9 (2016) 5791–5796.
[16] Z.M. Ye, S.J. Dai, F.Q. Yan, L. Wang, J. Fang, Z.F. Fu, Y.Z. Wang, DCE-MRI-derived volume transfer constant (K(trans)) and DWI apparent diffusion coefficient as predictive markers of short- and long-term efficacy of chemoradiotherapy in patients with esophageal cancer, Technol. Cancer Res. Treat. 17 (2018) 1533034618765254.
[17] M.W. Huellner, P. Appenzeller, F.P. Kuhn, L. Husmann, C.M. Pietsch, I.A. Burger, M. Porto, G. Delso, G.K. von Schulthess, P. Veit-Haibach, Whole-body nonenhanced PET/MR versus PET/CT in the staging and restaging of cancers: preliminary observations, Radiology 273 (3) (2014) 859–869.
[18] G. Lee, H.I.S.J. Kim, Y.J. Jeong, I.J. Kim, K. Pak, D.Y. Park, G.H. Kim, Clinical implication of PET/MR imaging in preoperative esophageal cancer staging: comparison with PET/CT, endoscopic ultrasonography, and CT, J. Nucl. Med. 55 (8) (2014) 1242–1247.
[19] C.S. Wong, N. Gong, Y.C. Chu, M.P. Anthony, Q. Chan, H.F. Lee, K.M. Chu, P.L. Khong, Correlation of measurements from diffusion weighted MR imaging and FDG PET/CT in GIST patients: ADC versus SUV, Eur. J. Radiol. 81 (9) (2012) 2122–2126.
[20] M. Regier, T. Derlin, D. Schwarz, A. Laqmani, F.O. Henes, M. Groth, J.H. Buhk, H. Kooijman, G. Adam, Diffusion weighted MRI and 18F-FDG PET/CT in non-small cell lung cancer (NSCLC): does the apparent diffusion coefficient (ADC) correlate with tracer uptake (SUV)? Eur. J. Radiol. 81 (10) (2012) 2913–2918.
[21] A. Wetter, C. Lipponer, F. Nensa, P. Heusch, H. Rubben, T.W. Schlosser, T.D. Poppel, T.C. Lauenstein, J. Nagarajah, Quantitative evaluation of bone metastases from prostate cancer with simultaneous [18F] choline PET/MRI: combined SUV and ADC analysis, Ann. Nucl. Med. 28 (5) (2014) 405–410.
[22] L. Goense, S.E. Heethuis, P.S.N. van Rossum, F.E.M. Voncken, J.J.W. Lagendijk, M. Lam, C.H. Terhaard, R. van Hillegersberg, J.P. Ruurda, S. Mook, A. van Lier, S.H. Lin, G.J. Meijer, Correlation between functional imaging markers derived from diffusion-weighted MRI and 18F-FDG PET/CT in esophageal cancer, Nucl. Med. Commun. 39 (1) (2018) 60–67.
[23] T. Aoyagi, K. Shuto, S. Okazumi, K. Hayano, A. Satoh, H. Saitoh, H. Shimada,

Y. Nabeya, T. Kazama, H. Matsubara, Apparent diffusion coefficient correlation with oesophageal tumour stroma and angiogenesis, Eur. Radiol. 22 (6) (2012) 1172–1177.
[24] S. Liu, H. Wang, W. Guan, L. Pan, Z. Zhou, H. Yu, T. Liu, X. Yang, J. He, Z. Zhou, Preoperative apparent diffusion coefficient value of gastric cancer by diffusion-weighted imaging: correlations with postoperative TNM staging, J. Magn. Reson. Imaging 42 (3) (2015) 837–843.
[25] F. Giganti, A. Salerno, A. Ambrosi, D. Chiari, E. Orsenigo, A. Esposito, L. Albarello, E. Mazza, C. Staudacher, A. Del Maschio, F. De Cobelli, Prognostic utility of diffusion-weighted MRI in oesophageal cancer: is apparent diffusion coefficient a potential marker of tumour aggressiveness? Radiol. Med. 121 (3) (2016) 173–180.
[26] T. Aoyagi, K. Shuto, S. Okazumi, H. Shimada, T. Kazama, H. Matsubara, Apparent diffusion coefficient values measured by diffusion-weighted imaging predict chemoradiotherapeutic effect for advanced esophageal cancer, Dig. Surg. 28 (4) (2011) 252–257.
[27] B.E. Chatterton, I. Ho Shon, A. Baldey, N. Lenzo, A. Patrikeos, B. Kelley, D. Wong, J.E. Ramshaw, A.M. Scott, Positron emission tomography changes management and prognostic stratification in patients with oesophageal cancer: results of a multicentre prospective study, Eur. J. Nucl. Med. Mol. Imaging 36 (3) (2009) 354–361.
[28] J.M. Omloo, G.W. Sloof, R. Boellaard, O.S. Hoekstra, P.L. Jager, H.M. van Dullemen, P. Fockens, J.T. Plukker, J.J. van Lanschot, Importance of fluorodeoxyglucose-positron emission tomography (FDG-PET) and endoscopic ultrasonography parameters in predicting survival following surgery for esophageal cancer, Endoscopy 40 (6) (2008) 464–471.
[29] M. Soret, S.L. Bacharach, I. Buvat, Partial-volume effect in PET tumor imaging, J. Nucl. Med. 48 (6) (2007) 932–945.
[30] M. Soussan, J. Cyrta, C. Pouliquen, K. Chouahnia, F. Orlhac, E. Martinod, V. Eder, J.F. Morere, I. Buvat, Fluorine 18 fluorodeoxyglucose PET/CT volume-based indices in locally advanced non-small cell lung cancer: prediction of residual viable tumor after induction chemotherapy, Radiology 272 (3) (2014) 875–884.
[31] J. Davison, G. Mercier, G. Russo, R.M. Subramaniam, PET-based primary tumor volumetric parameters and survival of patients with non-small cell lung carcinoma, AJR Am. J. Roentgenol. 200 (3) (2013) 635–640.
[32] K.P. Chang, N.M. Tsang, C.T. Liao, C.L. Hsu, M.J. Chung, C.W. Lo, S.C. Chan, S.H. Ng, H.M. Wang, T.C. Yen, Prognostic significance of 18F-FDG PET parameters and plasma Epstein-Barr virus DNA load in patients with nasopharyngeal carcinoma, J. Nucl. Med. 53 (1) (2012) 21–28.
[33] E.H. Dibble, A.C. Alvarez, M.T. Truong, G. Mercier, E.F. Cook, R.M. Subramaniam, 18F-FDG metabolic tumor volume and total glycolytic activity of oral cavity and oropharyngeal squamous cell cancer: adding value to clinical staging, J. Nucl. Med. 53 (5) (2012) 709–715.
[34] V. Malik, C. Johnston, D. O'Toole, J. Lucey, N. O'Farrell, Z. Claxton, J.V. Reynolds, Metabolic tumor volume provides complementary prognostic information to EUS staging in esophageal and junctional cancer, Dis. Esophagus 30 (3) (2017) 1–8.
[35] A. Surov, P. Stumpp, H.J. Meyer, M. Gawlitza, A.K. Hohn, A. Boehm, O. Sabri, T. Kahn, S. Purz, Simultaneous (18)F-FDG-PET/MRI: associations between diffusion, glucose metabolism and histopathological parameters in patients with head and neck squamous cell carcinoma, Oral Oncol. 58 (2016) 14–20.
[36] B.B. Chen, Y.W. Tien, M.C. Chang, M.F. Cheng, Y.T. Chang, C.H. Wu, X.J. Chen, T.C. Kuo, S.H. Yang, I.L. Shih, H.S. Lai, T.T. Shih, PET/MRI in pancreatic and periampullary cancer: correlating diffusion-weighted imaging, MR spectroscopy and glucose metabolic activity with clinical stage and prognosis, Eur. J. Nucl. Med. Mol. Imaging 43 (10) (2016) 1753–1764.